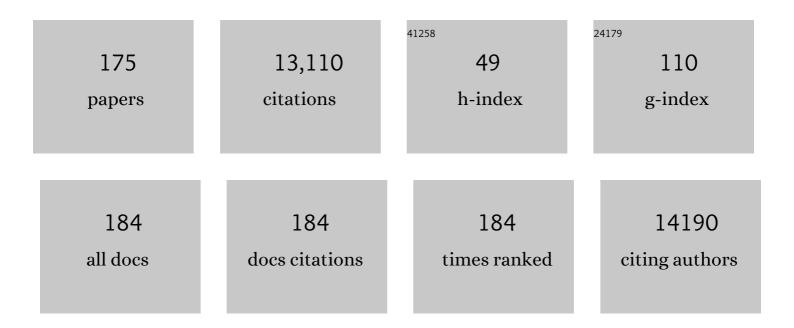
Jeffrey A Reimer

List of Publications by Year in descending order

Source: https://exaly.com/author-pdf/4402480/publications.pdf Version: 2024-02-01



#	Article	IF	CITATIONS
1	Characterization of Chemisorbed Species and Active Adsorption Sites in Mg–Al Mixed Metal Oxides for High-Temperature CO ₂ Capture. Chemistry of Materials, 2022, 34, 3893-3901.	3.2	10
2	A molecular perspective on carbon capture. Matter, 2022, 5, 1330-1333.	5.0	2
3	Electric-Field-Induced Spatially Dynamic Heterogeneity of Solvent Motion and Cation Transference in Electrolytes. Physical Review Letters, 2022, 128, .	2.9	17
4	Covalent Organic Frameworks with Irreversible Linkages via Reductive Cyclization of Imines. Journal of the American Chemical Society, 2022, 144, 9827-9835.	6.6	39
5	Nuclear spin temperature reversal via continuous radio-frequency driving. Physical Review B, 2021, 103, .	1.1	3
6	Magnetic field induced delocalization in hybrid electron-nuclear spin ensembles. Physical Review B, 2021, 103, .	1.1	6
7	Improved Li ⁺ Transport in Polyacetal Electrolytes: Conductivity and Current Fraction in a Series of Polymers. ACS Energy Letters, 2021, 6, 1886-1891.	8.8	36
8	Background-free dual-mode optical and ¹³ C magnetic resonance imaging in diamond particles. Proceedings of the National Academy of Sciences of the United States of America, 2021, 118, .	3.3	13
9	Modifying Li ⁺ and Anion Diffusivities in Polyacetal Electrolytes: A Pulsed-Field-Gradient NMR Study of Ion Self-Diffusion. Chemistry of Materials, 2021, 33, 4915-4926.	3.2	21
10	Observation of an Intermediate to H ₂ Binding in a Metal–Organic Framework. Journal of the American Chemical Society, 2021, 143, 14884-14894.	6.6	32
11	Origin of enhanced water oxidation activity in an iridium single atom anchored on NiFe oxyhydroxide catalyst. Proceedings of the National Academy of Sciences of the United States of America, 2021, 118, .	3.3	71
12	Overcoming Metastable CO ₂ Adsorption in a Bulky Diamine-Appended Metal–Organic Framework. Journal of the American Chemical Society, 2021, 143, 15258-15270.	6.6	51
13	Exploring the Ion Solvation Environments in Solid-State Polymer Electrolytes through Free-Energy Sampling. Macromolecules, 2021, 54, 8590-8600.	2.2	3
14	Low-field microwave-mediated optical hyperpolarization in optically pumped diamond. Journal of Magnetic Resonance, 2021, 331, 107021.	1.2	2
15	Chemically Stable Polyarylether-Based Metallophthalocyanine Frameworks with High Carrier Mobilities for Capacitive Energy Storage. Journal of the American Chemical Society, 2021, 143, 17701-17707.	6.6	42
16	Imaging Sequences for Hyperpolarized Solids. Molecules, 2021, 26, 133.	1.7	1
17	Solution-processable and functionalizable ultra-high molecular weight polymers via topochemical synthesis. Nature Communications, 2021, 12, 6818.	5.8	30
18	Precise Control of Molecular Selfâ€Diffusion in Isoreticular and Multivariate Metalâ€Organic Frameworks. ChemPhysChem, 2020, 21, 32-35.	1.0	29

#	Article	IF	CITATIONS
19	Cooperative Carbon Dioxide Adsorption in Alcoholamine―and Alkoxyalkylamineâ€Functionalized Metal–Organic Frameworks. Angewandte Chemie - International Edition, 2020, 59, 19468-19477.	7.2	58
20	Designing hierarchical nanoporous membranes for highly efficient gas adsorption and storage. Science Advances, 2020, 6, .	4.7	41
21	Enhanced Optical 13 C Hyperpolarization in Diamond Treated by Highâ€Temperature Rapid Thermal Annealing. Advanced Quantum Technologies, 2020, 3, 2000050.	1.8	8
22	Cooperative carbon capture and steam regeneration with tetraamine-appended metal–organic frameworks. Science, 2020, 369, 392-396.	6.0	249
23	Selective, High-Temperature O ₂ Adsorption in Chemically Reduced, Redox-Active Iron-Pyrazolate Metal–Organic Frameworks. Journal of the American Chemical Society, 2020, 142, 14627-14637.	6.6	32
24	Hydrological limits to carbon capture and storage. Nature Sustainability, 2020, 3, 658-666.	11.5	63
25	Optically pumped spin polarization as a probe of many-body thermalization. Science Advances, 2020, 6, .	4.7	18
26	Employing a Narrow-Band-Gap Mediator in Ternary Solar Cells for Enhanced Photovoltaic Performance. ACS Applied Materials & Interfaces, 2020, 12, 16387-16393.	4.0	22
27	Reversible Interlayer Sliding and Conductivity Changes in Adaptive Tetrathiafulvalene-Based Covalent Organic Frameworks. ACS Applied Materials & Interfaces, 2020, 12, 19054-19061.	4.0	40
28	Room temperature " <i>optical nanodiamond hyperpolarizer</i> ― Physics, design, and operation. Review of Scientific Instruments, 2020, 91, 023106.	0.6	24
29	Cooperative Carbon Dioxide Adsorption in Alcoholamine―and Alkoxyalkylamineâ€Functionalized Metal–Organic Frameworks. Angewandte Chemie, 2020, 132, 19636-19645.	1.6	5
30	Dynamic Covalent Synthesis of Crystalline Porous Graphitic Frameworks. CheM, 2020, 6, 933-944.	5.8	123
31	Influence of Pore Size on Carbon Dioxide Diffusion in Two Isoreticular Metal–Organic Frameworks. Chemistry of Materials, 2020, 32, 3570-3576.	3.2	29
32	Revealing Molecular Mechanisms in Hierarchical Nanoporous Carbon via Nuclear Magnetic Resonance. Matter, 2020, 3, 2093-2107.	5.0	34
33	Selective nitrogen adsorption via backbonding in a metal–organic framework with exposed vanadium sites. Nature Materials, 2020, 19, 517-521.	13.3	121
34	10.1063/1.5131655.1., 2020, , .		0
35	Water Enables Efficient CO ₂ Capture from Natural Gas Flue Emissions in an Oxidation-Resistant Diamine-Appended Metal–Organic Framework. Journal of the American Chemical Society, 2019, 141, 13171-13186.	6.6	107
36	Reticular Synthesis of Multinary Covalent Organic Frameworks. Journal of the American Chemical Society, 2019, 141, 11420-11424.	6.6	126

#	Article	IF	CITATIONS
37	Double Perovskite Structure Induced by Co Addition to PbTiO ₃ : Insights from DFT and Experimental Solid-State NMR Spectroscopy. Journal of Physical Chemistry C, 2019, 123, 27132-27139.	1.5	8
38	Carbon-13 dynamic nuclear polarization in diamond via a microwave-free integrated cross effect. Proceedings of the National Academy of Sciences of the United States of America, 2019, 116, 18334-18340.	3.3	20
39	Dynamics of frequency-swept nuclear spin optical pumping in powdered diamond at low magnetic fields. Proceedings of the National Academy of Sciences of the United States of America, 2019, 116, 2512-2520.	3.3	28
40	Wide dynamic range magnetic field cycler: Harnessing quantum control at low and high fields. Review of Scientific Instruments, 2019, 90, 013112.	0.6	11
41	Multistep Solid-State Organic Synthesis of Carbamate-Linked Covalent Organic Frameworks. Journal of the American Chemical Society, 2019, 141, 11253-11258.	6.6	92
42	Iron detection and remediation with a functionalized porous polymer applied to environmental water samples. Chemical Science, 2019, 10, 6651-6660.	3.7	30
43	Temperature-dependent interchromophoric interaction in a fluorescent pyrene-based metal–organic framework. Chemical Science, 2019, 10, 6140-6148.	3.7	45
44	Combined Nuclear Magnetic Resonance and Molecular Dynamics Study of Methane Adsorption in M ₂ (dobdc) Metal–Organic Frameworks. Journal of Physical Chemistry C, 2019, 123, 12286-12295.	1.5	18
45	Two-Electron-Spin Ratchets as a Platform for Microwave-Free Dynamic Nuclear Polarization of Arbitrary Material Targets. Nano Letters, 2019, 19, 2389-2396.	4.5	14
46	Dissolution of Lithium Metal in Poly(ethylene oxide). ACS Energy Letters, 2019, 4, 903-907.	8.8	28
47	Amine Dynamics in Diamine-Appended Mg ₂ (dobpdc) Metal–Organic Frameworks. Journal of Physical Chemistry Letters, 2019, 10, 7044-7049.	2.1	18
48	Data-driven design of metal–organic frameworks for wet flue gas CO2 capture. Nature, 2019, 576, 253-256.	13.7	438
49	Hyperpolarized relaxometry based nuclear T1 noise spectroscopy in diamond. Nature Communications, 2019, 10, 5160.	5.8	31
50	Identification of the strong BrÃ,nsted acid site in a metal–organic framework solid acid catalyst. Nature Chemistry, 2019, 11, 170-176.	6.6	198
51	Detection of the Order-to-Disorder Transition in Block Copolymer Electrolytes Using Quadrupolar 7Li NMR Splitting. ACS Macro Letters, 2019, 8, 107-112.	2.3	1
52	Unexpected Diffusion Anisotropy of Carbon Dioxide in the Metal–Organic Framework Zn ₂ (dobpdc). Journal of the American Chemical Society, 2018, 140, 1663-1673.	6.6	64
53	NMR Spectroscopy Reveals Adsorbate Binding Sites in the Metal–Organic Framework UiO-66(Zr). Journal of Physical Chemistry C, 2018, 122, 8295-8305.	1.5	33
54	Carbon capture and storage (CCS): the way forward. Energy and Environmental Science, 2018, 11, 1062-1176.	15.6	2,378

#	Article	IF	CITATIONS
55	Elucidating CO ₂ Chemisorption in Diamine-Appended Metal–Organic Frameworks. Journal of the American Chemical Society, 2018, 140, 18016-18031.	6.6	107
56	Crystalline Dioxin-Linked Covalent Organic Frameworks from Irreversible Reactions. Journal of the American Chemical Society, 2018, 140, 12715-12719.	6.6	289
57	Enhanced dynamic nuclear polarization via swept microwave frequency combs. Proceedings of the National Academy of Sciences of the United States of America, 2018, 115, 10576-10581.	3.3	45
58	Solid-State NMR Investigations of Carbon Dioxide Gas in Metal–Organic Frameworks: Insights into Molecular Motion and Adsorptive Behavior. Chemical Reviews, 2018, 118, 10033-10048.	23.0	93
59	Orientation-independent room temperature optical ¹³ C hyperpolarization in powdered diamond. Science Advances, 2018, 4, eaar5492.	4.7	91
60	Revisiting Anisotropic Diffusion of Carbon Dioxide in the Metal–Organic Framework Zn ₂ (dobpdc). Journal of Physical Chemistry C, 2018, 122, 15344-15351.	1.5	15
61	Highly effective ammonia removal in a series of BrÃ̧nsted acidic porous polymers: investigation of chemical and structural variations. Chemical Science, 2017, 8, 4399-4409.	3.7	89
62	Translational and Rotational Motion of C8 Aromatics Adsorbed in Isotropic Porous Media (MOF-5): NMR Studies and MD Simulations. Journal of Physical Chemistry C, 2017, 121, 15456-15462.	1.5	25
63	Enantioselective Recognition of Ammonium Carbamates in a Chiral Metal–Organic Framework. Journal of the American Chemical Society, 2017, 139, 16000-16012.	6.6	82
64	Uncovering the Local Magnesium Environment in the Metal–Organic Framework Mg2(dobpdc) Using 25Mg NMR Spectroscopy. Journal of Physical Chemistry C, 2017, 121, 19938-19945.	1.5	16
65	A Diaminopropane-Appended Metal–Organic Framework Enabling Efficient CO ₂ Capture from Coal Flue Gas via a Mixed Adsorption Mechanism. Journal of the American Chemical Society, 2017, 139, 13541-13553.	6.6	206
66	The Chemistry of CO ₂ Capture in an Amine-Functionalized Metal–Organic Framework under Dry and Humid Conditions. Journal of the American Chemical Society, 2017, 139, 12125-12128.	6.6	371
67	Following the structure and reactivity of Tuncbilek lignite during pyrolysis and hydrogenation. Fuel Processing Technology, 2016, 152, 266-273.	3.7	17
68	Chemical Conversion of Linkages in Covalent Organic Frameworks. Journal of the American Chemical Society, 2016, 138, 15519-15522.	6.6	373
69	Copper Capture in a Thioether-Functionalized Porous Polymer Applied to the Detection of Wilson's Disease. Journal of the American Chemical Society, 2016, 138, 7603-7609.	6.6	137
70	A Molecular Surface Functionalization Approach to Tuning Nanoparticle Electrocatalysts for Carbon Dioxide Reduction. Journal of the American Chemical Society, 2016, 138, 8120-8125.	6.6	340
71	Influence of magnetic field alignment and defect concentration on nitrogen-vacancy polarization in diamond. New Journal of Physics, 2016, 18, 013011.	1.2	26
72	The phenomenology of optically pumped 13C NMR in diamond at 7.05 T: Room temperature polarization, orientation dependence, and the effect of defect concentration on polarization dynamics. Journal of Magnetic Resonance, 2016, 264, 154-162.	1.2	19

#	Article	IF	CITATIONS
73	Nanoporous Materials Can Tune the Critical Point of a Pure Substance. Angewandte Chemie - International Edition, 2015, 54, 14349-14352.	7.2	16
74	NMR relaxation and exchange in metal–organic frameworks for surface area screening. Microporous and Mesoporous Materials, 2015, 205, 65-69.	2.2	14
75	Cooperative insertion of CO2 in diamine-appended metal-organic frameworks. Nature, 2015, 519, 303-308.	13.7	1,026
76	Anodic Oxidation of COads Derived from Methanol on Pt Electrocatalysts Linked to the Bonding Type and Adsorption Site. Electrochimica Acta, 2014, 135, 249-254.	2.6	1
77	Metal–Organic Frameworks with Precisely Designed Interior for Carbon Dioxide Capture in the Presence of Water. Journal of the American Chemical Society, 2014, 136, 8863-8866.	6.6	369
78	Electrochemical characterization of hydrogen-bonding complexation between indoline and nitrogen containing bases. Journal of Electroanalytical Chemistry, 2013, 691, 57-65.	1.9	5
79	Mapping of Functional Groups in Metal-Organic Frameworks. Science, 2013, 341, 882-885.	6.0	411
80	Understanding CO ₂ Dynamics in Metal–Organic Frameworks with Open Metal Sites. Angewandte Chemie - International Edition, 2013, 52, 4410-4413.	7.2	160
81	Solid state NMR investigation of Î ³ -irradiated composite siloxanes: Probing the silica/polysiloxane interface. Polymer Degradation and Stability, 2013, 98, 1362-1368.	2.7	8
82	In Situ Formation of Wilkinson-Type Hydroformylation Catalysts: Insights into the Structure, Stability, and Kinetics of Triphenylphosphine- and Xantphos-Modified Rh/SiO ₂ . ACS Catalysis, 2013, 3, 348-357.	5.5	36
83	Near-band-gap photoinduced nuclear spin dynamics in semi-insulating GaAs: Hyperfine- and quadrupolar-driven relaxation. Physical Review B, 2013, 88, .	1.1	4
84	Exâ€Situ NMR Relaxometry of Metal–Organic Frameworks for Rapid Surfaceâ€Area Screening. Angewandte Chemie, 2013, 125, 12265-12268.	1.6	8
85	Exâ€Situ NMR Relaxometry of Metal–Organic Frameworks for Rapid Surfaceâ€Area Screening. Angewandte Chemie - International Edition, 2013, 52, 12043-12046.	7.2	36
86	Effect of Confinement on Proton Transport Mechanisms in Block Copolymer/Ionic Liquid Membranes. Macromolecules, 2012, 45, 3112-3120.	2.2	74
87	CO ₂ Dynamics in a Metal–Organic Framework with Open Metal Sites. Journal of the American Chemical Society, 2012, 134, 14341-14344.	6.6	278
88	Utility of a tuneless plug and play transmission line probe. Journal of Magnetic Resonance, 2012, 221, 117-119.	1.2	10
89	Proton Hopping and Long-Range Transport in the Protic Ionic Liquid [Im][TFSI], Probed by Pulsed-Field Gradient NMR and Quasi-Elastic Neutron Scattering. Journal of Physical Chemistry B, 2012, 116, 8201-8209.	1.2	58
90	Optically rewritable patterns of nuclear magnetization in gallium arsenide. Nature Communications, 2012, 3, 918.	5.8	16

#	Article	IF	CITATIONS
91	High-Resolution NMR in Inhomogeneous Fields. , 2011, , 143-164.		0
92	Suppression of probe background signals via B1 field inhomogeneity. Journal of Magnetic Resonance, 2011, 209, 300-305.	1.2	11
93	Helicity independent optically-pumped nuclear magnetic resonance in gallium arsenide. Applied Physics Letters, 2011, 98, 112101.	1.5	5
94	Nuclear hyperpolarization in solids and the prospects for nuclear spintronics. Solid State Nuclear Magnetic Resonance, 2010, 37, 3-12.	1.5	40
95	Optical pumping of nuclear spin magnetization in GaAs/AlAs quantum wells of variable electron density. Solid State Communications, 2010, 150, 450-453.	0.9	4
96	Optical polarization of <mml:math <br="" xmlns:mml="http://www.w3.org/1998/Math/MathML">display="inline"><mml:mrow><mml:mmultiscripts><mml:mtext>C</mml:mtext><mml:mprescripts /><mml:none /><mml:mrow><mml:mn>13</mml:mn></mml:mrow></mml:none </mml:mprescripts </mml:mmultiscripts></mml:mrow></mml:math> nuclei in diamond through nitrogen vacancy centers. Physical Review B, 2010, 81, .	1.1	43
97	Modeling 1H NMR transverse magnetization decay in polysiloxane-silica composites. Chemical Engineering Science, 2009, 64, 4684-4692.	1.9	12
98	Electro-oxidation kinetics of adsorbed CO on platinum electrocatalysts. Chemical Engineering Science, 2009, 64, 4765-4771.	1.9	6
99	â€~Ex situ' magnetic resonance volume imaging. Chemical Physics Letters, 2009, 467, 398-401.	1.2	2
100	Active-Site Motions and Polarity Enhance Catalytic Turnover of Hydrated Subtilisin Dissolved in Organic Solvents. Journal of the American Chemical Society, 2009, 131, 4294-4300.	6.6	31
101	Proton conduction and characterization of an La(PO3)3–Ca(PO3)2 glass–ceramic. Solid State Ionics, 2008, 178, 1811-1816.	1.3	20
102	A Methodology for the Indirect Determination and Spatial Resolution of Shear Modulus of PDMSâ^'Silica Elastomers. Macromolecules, 2008, 41, 1323-1327.	2.2	7
103	Site-Dependent ¹³ C Chemical Shifts of CO Adsorbed on Pt Electrocatalysts. Journal of Physical Chemistry C, 2008, 112, 14702-14705.	1.5	6
104	Biocatalyst activity in nonaqueous environments correlates with centisecond-range protein motions. Proceedings of the National Academy of Sciences of the United States of America, 2008, 105, 15672-15677.	3.3	30
105	Penetration depth model for optical alignment of nuclear spins in GaAs. Physical Review B, 2007, 76, .	1.1	15
106	Characterizing electrocatalytic surfaces: Electrochemical and NMR studies of methanol and carbon monoxide on Pt/C. Electrochimica Acta, 2007, 53, 1365-1371.	2.6	9
107	Portable, low-cost NMR with laser-lathe lithography produced microcoils. Journal of Magnetic Resonance, 2007, 189, 121-129.	1.2	53
108	Covalency Measurements via NMR in Lithium Metal Phosphates. Applied Magnetic Resonance, 2007, 32, 547-563.	0.6	49

#	Article	IF	CITATIONS
109	An effective stochastic excitation strategy for finding elusive NMR signals from solids. Solid State Nuclear Magnetic Resonance, 2006, 29, 199-203.	1.5	5
110	Toward ex situ phase-encoded spectroscopic imaging. Concepts in Magnetic Resonance Part B, 2006, 29B, 137-144.	0.3	8
111	Water dynamics and salt-activation of enzymes in organic media: Mechanistic implications revealed by NMR spectroscopy. Proceedings of the National Academy of Sciences of the United States of America, 2006, 103, 5706-5710.	3.3	49
112	Investigation of particle isolation in Li-ion battery electrodes using 7Li NMR spectroscopy. Electrochemistry Communications, 2005, 7, 1249-1251.	2.3	25
113	Photocurrent-modulated optical nuclear polarization in bulk GaAs. Applied Physics Letters, 2005, 87, 232109.	1.5	8
114	Nuclear spin temperature and magnetization transport in laser-enhanced NMR of bulk GaAs. Physical Review B, 2005, 71, .	1.1	24
115	Layered Nickel Oxide-Based Cathodes for Lithium Cells: Analysis of Performance Loss Mechanisms. Journal of the Electrochemical Society, 2005, 152, A1629.	1.3	14
116	High-Resolution NMR Spectroscopy with a Portable Single-Sided Sensor. Science, 2005, 308, 1279-1279.	6.0	142
117	Optical polarization of nuclear spins in GaAs. Physical Review B, 2004, 69, .	1.1	43
118	Mechanism of Lithium Insertion into Magnesium Silicide. Journal of the Electrochemical Society, 2004, 151, A493.	1.3	26
119	Three-dimensional phase-encoded chemical shift MRI in the presence of inhomogeneous fields. Proceedings of the National Academy of Sciences of the United States of America, 2004, 101, 8845-8847.	3.3	24
120	Diagnostic Analysis of Electrodes from High-Power Lithium-Ion Cells Cycled under Different Conditions. Journal of the Electrochemical Society, 2004, 151, A857.	1.3	54
121	Nitrous oxide decomposition and surface oxygen formation on Fe-ZSM-5. Journal of Catalysis, 2004, 224, 148-155.	3.1	106
122	Methanol formation on Fe/Al-MFI via the oxidation of methane by nitrous oxide. Journal of Catalysis, 2004, 225, 300-306.	3.1	137
123	Internal combustion. Nature, 2003, 426, 508-509.	13.7	7
124	Influence of Substitution on the Structure and Electrochemistry of Layered Manganese Oxides. Chemistry of Materials, 2003, 15, 4456-4463.	3.2	44
125	NMR Studies of Structural Phase Transitions in Random Copolymers. Macromolecules, 2003, 36, 477-485.	2.2	1
126	Sulfur-Doped Aluminum-Substituted Manganese Oxide Spinels for Lithium-Ion Battery Applications. Journal of the Electrochemical Society, 2003, 150, A1060.	1.3	7

#	Article	IF	CITATIONS
127	An Electrochemical and XRD Study of Lithium Insertion into Mechanically Alloyed Magnesium Stannide. Journal of the Electrochemical Society, 2003, 150, A912.	1.3	11
128	The use of a permanent magnet for water content measurements of wood chips. IEEE Transactions on Applied Superconductivity, 2002, 12, 975-978.	1.1	9
129	A [sup 7]Li NMR Study of Capacity Fade in Metal-Substituted Lithium Manganese Oxide Spinels. Journal of the Electrochemical Society, 2002, 149, A574.	1.3	36
130	[sup 7]Li and [sup 31]P Magic Angle Spinning Nuclear Magnetic Resonance of LiFePO[sub 4]-Type Materials. Electrochemical and Solid-State Letters, 2002, 5, A95.	2.2	74
131	The Influence of Covalence on Capacity Retention in Metal-Substituted Spinels. Journal of the Electrochemical Society, 2002, 149, A1409.	1.3	20
132	Hyperfine Fields at the Li Site in LiFePO4-Type Olivine Materials for Lithium Rechargeable Batteries:Â A7Li MAS NMR and SQUID Study. Journal of the American Chemical Society, 2002, 124, 3832-3833.	6.6	107
133	Magnesium silicide as a negative electrode material for lithium-ion batteries. Journal of Power Sources, 2002, 110, 424-429.	4.0	103
134	Cadmium Solid State NMR Studies of Cadmium-Exchanged Zeolites. Catalysis Letters, 2002, 80, 19-24.	1.4	4
135	Properties of GaAs nanoclusters deposited by a femtosecond laser. Journal of Materials Science, 2002, 37, 3953-3958.	1.7	23
136	Nuclear Magnetic Resonance and Voltammetry Studies of Carbon Monoxide Adsorption and Oxidation on a Carbon-Supported Platinum Fuel Cell Electrocatalyst. Journal of the Electrochemical Society, 2001, 148, A137.	1.3	53
137	Solid-State NMR Studies of Lead-Containing Zeolites. Journal of Physical Chemistry B, 2001, 105, 2945-2950.	1.2	13
138	Towards more active biocatalysts in organic media: Increasing the activity of salt-activated enzymes. Biotechnology and Bioengineering, 2001, 75, 187-196.	1.7	50
139	A [sup 7]Li Nuclear Magnetic Resonance Study of Metal-Substituted Lithium Manganese Oxide Spinels. Journal of the Electrochemical Society, 2001, 148, A951.	1.3	17
140	On the Salt-Induced Activation of Lyophilized Enzymes in Organic Solvents:Â Effect of Salt Kosmotropicity on Enzyme Activity. Journal of the American Chemical Society, 2000, 122, 1565-1571.	6.6	135
141	GaAs nanostructures and films deposited by a Cu-vapor laser. Applied Physics Letters, 1999, 75, 2208-2210.	1.5	6
142	An in situ infrared study of NO reduction by C3H8 over Feâ€ZSMâ€5. Catalysis Letters, 1999, 63, 233-240.	1.4	115
143	Optimizing the salt-induced activation of enzymes in organic solvents: Effects of lyophilization time and water content. , 1999, 63, 233-241.		98
144	Structure and Density of Mo and Acid Sites in Mo-Exchanged H-ZSM5 Catalysts for Nonoxidative Methane Conversion. Journal of Physical Chemistry B, 1999, 103, 5787-5796.	1.2	303

#	Article	IF	CITATIONS
145	Multinuclear NMR study of enzyme hydration in an organic solvent. , 1998, 57, 686-693.		39
146	Supertransferred Hyperfine Fields at7Li:Â Variable Temperature7Li NMR Studies of LiMn2O4-Based Spinels. Journal of Physical Chemistry B, 1998, 102, 10142-10149.	1.2	70
147	Single-input double-tuned circuit for double resonance nuclear magnetic resonance experiments. Review of Scientific Instruments, 1998, 69, 477-478.	0.6	15
148	Multinuclear NMR study of enzyme hydration in an organic solvent. Biotechnology and Bioengineering, 1998, 57, 686-93.	1.7	10
149	Optical Pumping in Solid State Nuclear Magnetic Resonance. The Journal of Physical Chemistry, 1996, 100, 13240-13250.	2.9	79
150	Quantitative Solid-State NMR Spectra of CO Adsorbed from Aqueous Solution onto a Commercial Electrode. Journal of the American Chemical Society, 1996, 118, 12250-12251.	6.6	41
151	High-field cross polarization NMR from laser-polarized xenon to surface nuclei. Applied Magnetic Resonance, 1995, 8, 373-384.	0.6	40
152	Dynamic Monte Carlo simulation of spinâ€lattice relaxation of quadrupolar nuclei in solids. Oxygenâ€17 in yttriaâ€doped ceria. Journal of Chemical Physics, 1993, 98, 7613-7620.	1.2	36
153	High-field cross polarization NMR from laser-polarized xenon to a polymer surface. Journal of the American Chemical Society, 1993, 115, 8491-8492.	6.6	87
154	Nuclear Magnetic Resonance Studies of Deuterium in Silicon. Materials Research Society Symposia Proceedings, 1992, 262, 443.	0.1	0
155	A simple model for the etching of photoresist with plasmaâ€generated reactants. Journal of Applied Physics, 1992, 72, 5081-5088.	1.1	14
156	Enhancement of Photoresist Etch Rates by Argon Metastables in a Plasma Afterglow Reactor. Materials Research Society Symposia Proceedings, 1991, 236, 199.	0.1	1
157	Anomalous etch rates of photoresist with argon dilution of CF4/O2plasma afterglows. Applied Physics Letters, 1991, 59, 1547-1549.	1.5	4
158	A compact, high temperature nuclear magnetic resonance probe for use in a narrowâ€bore superconducting magnet. Review of Scientific Instruments, 1990, 61, 3368-3371.	0.6	7
159	Silane pyrolysis in a piston reactor. AICHE Journal, 1989, 35, 793-802.	1.8	15
160	Structure and optical properties of plasmaâ€deposited fluorinated silicon nitride thin films. Journal of Applied Physics, 1988, 63, 2651-2659.	1.1	19
161	Deposition Chemistry and Structure of Amorphous Fluorinated Silicon Nitride. Materials Research Society Symposia Proceedings, 1988, 118, 67.	0.1	2
162	Influence of Degree of Polymerization on Phase Separation and Rheology of A Thermotropic Liquid Crystal Polymer. Molecular Crystals and Liquid Crystals Incorporating Nonlinear Optics, 1987, 153, 271-280.	0.3	1

#	Article	IF	CITATIONS
163	A nuclear magnetic resonance study of phosphorusâ€doped polycrystalline silicon. Journal of Applied Physics, 1987, 62, 3665-3670.	1.1	3
164	Monte Carlo simulations of amorphous hydrogenated silicon thinâ€film growth. Journal of Applied Physics, 1987, 61, 2866-2873.	1.1	42
165	Inhomogeneous carbon bonding in hydrogenated amorphous carbon films. Journal of Applied Physics, 1987, 61, 2874-2877.	1.1	128
166	Hydrogen Microstructure in Amorphous Semiconductors Materials Research Society Symposia Proceedings, 1987, 95, 171.	0.1	2
167	Identification of Chemical Growth Mechanisms in Amorphous Semiconductors. Materials Research Society Symposia Proceedings, 1987, 95, 209.	0.1	1
168	Carbon Local Bonding Configurations in Amorphous Hydrogenated Silicon-Carbon Alloys. Materials Research Society Symposia Proceedings, 1987, 95, 329.	0.1	1
169	A simple method to study gas phase reactions. AICHE Journal, 1987, 33, 2037-2046.	1.8	2
170	Amorphous Hydrogenated Semiconductors. Materials Research Society Symposia Proceedings, 1986, 68, 157.	0.1	0
171	Multiple Quantum NMR Study of Hydrogen Clustering in Amorphous Silicon. Materials Research Society Symposia Proceedings, 1986, 70, 83.	0.1	1
172	The Properties Of Phosphorus In Polycrystalline Silicon - A Nuclear Magnetic Resonance Study. Materials Research Society Symposia Proceedings, 1986, 71, 375.	0.1	1
173	A ²⁹ Si-NMR Investigation of Amorphous Hydrogenated Silicon Nitride. Materials Research Society Symposia Proceedings, 1986, 70, 337.	0.1	3
174	Multiple-Quantum NMR Study of Clustering in Hydrogenated Amorphous Silicon. Physical Review Letters, 1986, 56, 1377-1380.	2.9	209
175	NMR Studies ofortho andmeta- fluorocinnamate-α-chymotrypsin complexes. Magnetic Resonance in Chemistry, 1979, 12, 352-356.	0.7	5